NASA TECHNICAL NOTE

NASA TN D-3265

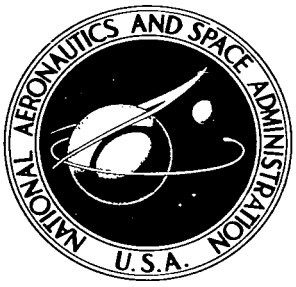

NASA TN D-3265

MEASUREMENTS OF RESONANT CHARGE EXCHANGE CROSS SECTIONS IN NITROGEN AND ARGON BETWEEN 0.5 AND 17 EV

by Billy J. Nichols and Fred C. Witteborn

Ames Research Center
Moffett Field, Calif.

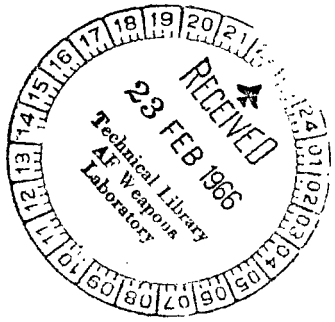

NATIONAL AERONAUTICS AND SPACE ADMINISTRATION • WASHINGTON, D. C. • FEBRUARY 1966

MEASUREMENTS OF RESONANT CHARGE EXCHANGE CROSS SECTIONS IN NITROGEN AND ARGON BETWEEN 0.5 AND 17 EV

By Billy J. Nichols and Fred C. Witteborn

Ames Research Center
Moffett Field, Calif.

NATIONAL AERONAUTICS AND SPACE ADMINISTRATION

For sale by the Clearinghouse for Federal Scientific and Technical Information
Springfield, Virginia 22151 – Price $2.00

MEASUREMENTS OF RESONANT CHARGE EXCHANGE CROSS SECTIONS IN NITROGEN AND ARGON BETWEEN 0.5 AND 17 EV

By Billy J. Nichols and Fred C. Witteborn
Ames Research Center

SUMMARY

The cross sections for charge transfer between N_2 molecules and N_2^+ ions and A atoms and A^+ ions have been determined within the energy range 0.5 to 17 eV. A knowledge of charge exchange cross sections of atmospheric ions in this energy range is required for calculating thermal conductivity and, to a lesser extent, other transport properties at high temperatures. While ions studied in this research are present in only small quantities in practical situations, measurements of their cross sections were useful in developing techniques for studying other ions and for comparing the results with theoretical calculations of resonant charge exchange cross sections. The variation of the cross section (σ) with energy (E) for each of these processes may be approximately represented by an expression of the form

$$\sigma^{1/2} = a - b \ln E$$

which is characteristic of symmetric resonance charge transfer. If E is measured in electron volts, then the values obtained for the nitrogen reaction were $a = 6.48\times10^{-8}$ cm, and $b = 0.24\times10^{-8}$ cm, and for the argon reaction $a = 7.49\times10^{-8}$ cm, and $b = 0.73\times10^{-8}$ cm.

Departures from the logarithmic behavior were noted in the nitrogen data, but not in the argon data. These differences consisted of a small hump at an incident ion energy of 8.5 eV and a steady increase of σ over the logarithmic expression below 3 eV. At 1 eV the measured cross section between N_2 and N_2^+ was 59×10^{-16} cm^2.

INTRODUCTION

Although a great deal of charge exchange data has been published for ion energies above 10 or 20 eV, almost none has been obtained between 0.5 and 10 eV. Unfortunately it is precisely in this region that aerodynamicists are most interested. Particle collisions at such energies predominate between 5,000° and 100,000° K, temperatures for which transport properties in gases must be known in order to predict the heating of vehicles entering the atmosphere at high speeds. The importance of charge exchange cross sections in calculating transport properties at high temperatures is discussed by Mason, Vanderslice, and Yos (ref. 1). Their theoretical paper predicts that charge exchange is often the dominant factor in thermal conduction. Techniques for

working in the desired energy range as well as for determining cross sections for two reactions already studied are described in this report.

Excellent surveys of cross-section data, techniques, and theory are given in recently published books by McDaniel (ref. 2) and Hasted (ref. 3). These also include extensive bibliographies. While almost no experimental values of charge exchange cross sections below 10 eV are available for collisions among atmospheric ions, theoretical predictions for some resonant reactions are available (refs. 4 and 5). Resonant reactions are those in which the total internal energy of the system is the same before and after the collision. This condition would be expected for the two reactions studied in this report:

$$N_2^+ + N_2 \rightarrow N_2 + N_2^+$$

and

$$A^+ + A \rightarrow A + A^+$$

Rapp and Francis (ref. 4) gave theoretical values of the argon reaction down to 1 eV. Dalgarno (ref. 6) used mobility data taken at 300° K to deduce low energy charge exchange cross sections (0.1 to 1000 eV) for argon and other atoms.

The lack of cross-section data at low energies is due to several experimental difficulties characteristic of work with low-energy ion beams. The most serious is spreading of the ion beam induced by the mutual repulsion of the ions. Even if the beam could be contained by some applied field, the space charge would cause the potential energy of ions at the center of the beam to differ from the energy of those near the edge. This would give rise to differences in the kinetic energy of particles in the beam and would result in loss of knowledge of the collision energy for the beam interacting with a gas. Thus the density of the ion beam current must be kept small enough that the variation in potential energy due to space charge across the beam is much smaller than the kinetic energy of the colliding particles. In practice this means a small ion current (e.g., 3×10^{-8} A) for 1 eV N_2^+ ions if their energy spread is to be less than 10 percent. The difficulties of working with small ion currents have been greatly alleviated in recent years through the development of better electrometers, the use of modulated beam techniques, and the use of single ion counting devices.

The low-energy ion beam faces difficulties other than space charge effects. It is readily affected by stray magnetic fields which must either be shielded from or incorporated in the guidance of the ions. Stray electric fields can be shielded to some extent, but contact potential differences exist even along grounded metal surfaces. If the target and other surfaces bounding the slow ion beam are coated with a uniform deposit of the proper conductor, contact potential differences may be reduced to values well below 0.1 V. The choice of material is important since even freshly evaporated films of some metals exhibit contact potential differences of a few tenths of a volt (ref. 7).

A difficulty in interpreting cross-section data at all energies is caused by the presence of excited ions in the beam. The effect has been studied

experimentally above 40 eV (refs. 8,9). In general, an excited ion will have a different charge exchange cross section than a ground state ion. Consider a slow excited molecular nitrogen ion N_2^{+*} colliding with the ground state molecule N_2. Two reactions are possible:

$$N_2^{+*} + N_2 \rightarrow N_2 + N_2^{+*}$$

$$N_2^{+*} + N_2 \rightarrow N_2^{*} + N_2^{+}$$

The first reaction is resonant and thus has a cross section that increases as the energy decreases. Its value need not be the same as that of the ground state reactants. The second is probably nonresonant. Its cross section would be zero at sufficiently low energy but would rise to a maximum somewhere in the the low energy range. Thus the presence of excited ions in the incident beam will lead to a cross section that is actually a mixture of cross sections of several different reactions.

A novel technique was used to measure charge exchange cross sections between 0.5 and 17 eV. A mass analyzed monoenergetic beam of ions was slowed down electrostatically to the desired energy and directed into a small reaction chamber in which the target gas pressure was high enough to charge exchange a significant fraction of the beam. In the reaction chamber, the beam was constrained by an axial magnetic field which caused all the ions moving toward the target (ion collector plate) to be measured as a current whether or not they had suffered collisions. The potential of the target was raised slightly so that the thermal ions formed by charge exchange in the reaction chamber could be repelled and thus distinguished from the faster ions of the incident beam. Charge exchange cross sections may be readily calculated from the measured currents of thermal and incident ions together with the known path length and pressure in the reaction chamber.

The apparatus and techniques for low-energy cross-section measurements are described in this report, along with the experimentally measured cross sections for the reactions

$$A^{+} + A \rightarrow A + A^{+}$$

and

$$N_2^{+} + N_2 \rightarrow N_2 + N_2^{+}$$

between 0.5 and 17 eV. The curves for cross section versus energy follow the expected

$$\sigma^{1/2} = a - b \ln E$$

form, except for some small humps in the nitrogen curves which are interpreted in terms of vibrationally excited incident ions.

measured inside the reaction chamber by a McLeod gage. These pressures were always below 10^{-3} torr, so that fast particles were likely to experience no more than one reaction.

Under conditions controlled as described above, the accelerator presently delivers 10^{-8} A of N_2^+ to a 1 cm^2 spot on the target at an energy of 10 eV with a total energy dispersion of 0.8 eV.

METHOD OF DATA ANALYSIS

Charge exchange cross sections were computed from the measured current due to the formation of slow ions upon passage of a fast ion beam through a thermal gas of known density. The current to the target consisted of the sum of the primary ions that did not suffer a collision, ions elastically scattered (within limits discussed later in this report) and 1/2 of the thermal ions that were formed through the charge exchange process. (The other thermal ions move away from the target because of their random motion.) The slow ion current was determined by measuring the drop in target current caused by application of a small retarding voltage, V_t, to the target relative to the reaction chamber. Typical plots of target current versus V_t are shown in figure 4(a) for pressures of 10^{-6} and 10^{-3} torr in the reaction chamber. As can be seen with the aid of the expanded voltage scale in figure 4(b), the drop in target current occurs for values of V_t between -0.1 V and +0.1 V. This drop then gives the current, I_s, due to 1/2 the slow ions formed. This current, I_s, was measured for each set of parameters (i.e., beam energy and reaction chamber pressure). The path length of the primary ions in the thermal gas was accurately defined by the distance between grid No. 2 and the target and held constant throughout the measurements. Ions formed outside the reaction chamber were attracted to grid No. 1 and thus did not introduce an error into the cross-section data. If we let I_f represent the target current with $V_t = 0.1$ V (i.e., the primary ion current) and I_o be the current at the entrance of the reaction chamber ($z = 0$), then the cross section may be calculated by using the beam attenuation formula

$$I_f = I_o \exp^{(-\sigma n z)}$$

which, since $I_o = I_f + 2I_s$, may be written

$$I_f = (I_f + 2I_s)\exp^{(-\sigma n z)} = (I_f + 2I_s)\exp^{(-\sigma z P/kT)}$$

where z is the path length of the ions in the thermal gas, $n = P/kT$ is the number density of the thermal gas, P is the absolute pressure in the reaction chamber, T is the absolute temperature of the reaction chamber walls, and k is Boltzmann's constant.

For each value of the ion beam energy, I_s was measured at four different pressures. Values of $\ln [I_f/(I_f + 2I_s)]$ were plotted as a function of relative pressure, and the slope of the curve was determined. Typical curves of this type are shown in figure 5. The path length z was measured directly,

and P was determined by calibrating the ion gage with McLeod gage measurements of the pressure inside the reaction chamber. Values of σ were then calculated by use of the equation

$$\sigma = C \frac{T}{z} (\text{slope})$$

where C is determined by the calibration of the ion gage. Each data point on the cross-section curves then is determined by measurements at four different pressure levels.

Since the primary ion beam energy was 18 eV or less, it was assumed that no secondary electrons were ejected from the metal surfaces. The coefficient for secondary electron emission from metal surfaces being struck by ions of 25 eV energy is expected to be on the order of 10^{-4}. In any case the plot of target current as a function of target voltage relative to the reaction chamber (see fig. 4(a)) should show this effect if it is present. As the target voltage is increased, grid No. 3 in effect becomes a secondary electron suppressor. The absence of a drop in current with a small voltage increase in the upper curve, figure 4(a), shows that if secondary electrons are emitted, they are too few to be detected and hence can be neglected.

RESULTS AND DISCUSSION

In order to understand the charge exchange data obtained for this report, it is important to note what happens to elastically scattered particles. In the following discussion we interpret the curves in figure 4(a). We then show that the measured charge exchange cross sections include nearly all the charge exchange whether accompanied by elastic scattering or not. It will be shown that they do not include elastic scattering unaccompanied by charge exchange, except for the presumably rare cases of large angle deflection.

The data in figures 4(a) and 4(b) show that as the target voltage was raised very slightly above the potential of the reaction chamber, the current dropped sharply. This was clearly due to repulsion of slow ions formed by charge exchange between the ambient gas in the chamber and the incident ions. Figure 4(a) also shows that no such drop in current occurred with only background gas ($P < 10^{-6}$ torr) in the chamber.

Since no momentum transfer needs to accompany the resonant reaction, most of the slow ions should have a thermal energy distribution appropriate to approximately 300° K, the wall temperature of the reaction chamber. As pointed out earlier, only half of the thermal ions would reach the collector, since at thermal equilibrium half the molecules are moving away from it. Differences in potential along the surface of the collector cause the drop in current versus retarding potential curve to be spread over a small voltage range (fig. 4(b)). Because of the presence of these contact potential differences the collector must be 0.1 V negative to measure all the slow ion current directed toward the collector and 0.1 V positive to repel that current. (Note that the closely spaced grid in front of the collector prevents this

field from penetrating the reaction chamber far enough to draw in the other half of the slow ions moving away from the collector.) Part of the broadening of the voltage range over which the slow ion current decreases results from the range of thermal energies, but at 300° K this is only about 0.03 eV - somewhat less than the expected contact potential differences.

Most of the runs showed an additional decrease of the target current as the retarding potential was increased above 0.1 V. This should give a measure of angular scattering, because scattered ions reach the detector with less axially directed kinetic energy. Indeed the entire retarding potential curve beyond $V = 0.1$ V is affected principally by angular scattering and the energy spread in the incident beam. Since the curve taken without gas in the chamber also reveals the energy dispersion in the incident beam, the effects of angular scattering may be isolated. Attenuation of the current by retarding potentials slightly above 0.1 V is directly proportional to the number of incident ions which have experienced charge exchange in addition to a small angle elastic collision, plus the number which have experienced large angle scattering without charge exchange (the latter number being negligible according to theory). Attenuation of the current near the end of the distribution ($V_t = 8$ V in fig. 4(a)) results from retardation of ions which have suffered large angle scattering with charge exchange or small angle scattering without charge exchange. The latter effect is expected to be dominant, but it is obscured by the energy dispersion in the beam. For this reason we have not yet attempted to make a quantitative estimate of differential scattering cross sections from our data. An additional complication arises from inelastic collisions. These would reduce the axial kinetic energy, but would be interpreted as purely elastic angular scattering in the method just described.

Consideration of Angular Scattering

We must now estimate the angular scattering which particles may suffer and still be included in the charge exchange measurement. The data for this report were obtained by comparing the current at $V_t = 0.1$ V with that at -0.1 V. Thus a neutral ambient gas molecule of N_2 or A initially at rest could pick up as much as 0.1 eV in the charge exchange collision and still be repelled by the retarding potential field. If the ambient molecule gained 0.1 eV, then the incident ion lost 0.1 eV in the collision. If we denote the transverse and axially directed energy of the incident ions by E_t and E_a, respectively, and the corresponding momenta by p_t and p_a, and use primes to denote these quantities after the collision, then by conservation of momentum,

$$p_a(1) = p_a'(1) + p_a'(2)$$

$$p_t'(1) = -p_t'(2)$$

and by conservation of energy,

$$E_a(1) = E_a'(1) + E_t'(1) + E_a'(2) + E_t'(2)$$

The (1) refers to the incident particle and the (2) to the struck particle. We are concerned with the case in which $E_a'(2) \leq 0.1$ eV. We wish to know the

maximum angle of deflection of the incident particle

$$\theta_{max} = \arctan p_t'(1)/p_a'(1)$$

Solution of the above equations using equal masses for incident and struck particles and the identity $p^2/2m = E$, yields after considerable algebra:

$$\theta_{max} = \arctan \frac{\{[E_a(1)E_a'(2)]^{1/2} - E_a'(2)\}^{1/2}}{[E_a(1)]^{1/2} - [E_a'(2)]^{1/2}}$$

If we let $R = E_a'(2)/E_a(1)$ then

$$\theta_{max} = \arctan \frac{(R^{1/2} - R)^{1/2}}{1 - R^{1/2}}$$

The angles θ_{max} for several incident ion energies appear in table I.

Since our measured cross sections are for charge exchange in which the incident particle was scattered by less than θ_{max} and since it is well known (ch. 4, ref. 2) that ion scattering is primarily in a forward direction at much smaller angles than θ_{max}, the values measured are essentially a total charge exchange cross section.

As mentioned above, the measured cross sections also include a contribution from ions scattered at large angles that did not experience charge exchange. We must calculate the minimum scattering angle that would permit such ions to be retarded by 0.1 V (i.e., $E_a'(1) \leq 0.1$ eV). Using the equations for conservation of energy and momentum we find

$$\frac{p_t'(1)}{p_a'(1)} = \frac{\{[E_a(1)E_a'(1)]^{1/2} - E_a'(1)\}^{1/2}}{[E_a'(1)]^{1/2}} = (Q^{1/2} - 1)^{1/2}$$

where $Q = E_a(1)/E_a'(1)$.

Then $\theta_{min} = \arctan (Q^{1/2} - 1)^{1/2}$. At $E_a(1) = 0.5$ eV, $\theta_{min} = 48^\circ$ and at 10 eV, 70.5°. While the angular scattering will be a subject of future investigation, it is inferred from experimental data on atoms at thermal energies (ref. 2) that scattering into angles greater than θ_{min} was negligible compared with the charge exchange process in the range of energies studied. Thus the measured cross sections are for charge exchange. They include charge exchange processes in which elastic scattering also took place. They do not include much elastic scattering without charge exchange.

Charge Exchange Cross Sections

Experimental values obtained for the charge exchange cross section of argon are listed in table II and shown graphically in figure 6(a). They are compared with other measurements and with theory in figure 6(b). The spread in our data is believed to result primarily from fluctuations in the beam current. The randomness of the fluctuations from a smooth curve suggests that there is no structure in the actual curve for cross section as a function of energy. As seen from figure 6(b) the cross sections may be described by the relation $\sigma^{1/2} = a - b \ln E$ with $a = 7.49 \times 10^{-8}$ cm and $b = 0.73 \times 10^{-8}$ cm. The good agreement with existing experimental data (refs. 11,12,13) and with theory (refs. 4,5) serves as a favorable check on our apparatus and method.

Since the argon ions were formed from 40 eV electrons, there is a possibility that some were in metastable states during the reaction. Experiments by Amme and Hayden (ref. 9) with argon ions formed from 16 to 40 eV electrons show a negligible effect of excited states on cross sections between ion energies of 50 and 1000 eV.

The measured values of the charge exchange cross section for the nitrogen reaction are listed in table III and shown graphically as a function of energy in figure 7(a). Comparison with an extrapolated curve (ref. 14) is made in figure 7(b) again using the relation $\sigma^{1/2} = a - b \ln E$ with $a = 6.48 \times 10^{-8}$ cm and $b = 0.24 \times 10^{-8}$ cm.

There appears to be a definite hump in the nitrogen curve at 8.5 eV. This peak will be shown to suggest the presence of a vibrationally excited state in the incident ion beam. In discussing Massey's adiabatic hypothesis as applied to nonresonant charge transfer, McDaniel (ref. 2) suggests that cross sections for such reactions should attain a peak value when the velocity of the incident particle is near $v = l\delta E/h$, where δE is the energy defect (i.e., the change in internal energy resulting from the reaction) and l is the adiabatic parameter for a large number of various interactions. Note that our observed peak came at $8.5 \text{ eV} = 1/2\ mv^2 = m[l^2(\Delta E)^2]/h^2$. The corresponding energy defect is 0.046 eV. This could easily be identified with either of the reactions

$$N_2^+(v = 2) + N_2(v = 0) \rightarrow N_2(v = 1) + N_2^+(v = 1) - 0.04 \text{ eV}$$

$$\rightarrow N_2(v = 2) + N_2^+(v = 0) + 0.06 \text{ eV}$$

which are mentioned by J. W. McGowan et al. (ref. 15) as possible nonresonant reactions in nitrogen charge exchange studies.

The increase in cross section above the $a - b \ln E$ curve at low energies may be due partly to elastic scattering. However, the absence of this departure from the logarithmic behavior in our argon data suggests that a real difference between actual and extrapolated nitrogen charge exchange cross sections has been found below 3 eV. The question will have to be decided by improved data of the type in figure 4(b) and by cross-section measurements at still lower energies.

Discussion of Errors

The accuracy of the cross sections may be determined from the accuracy of the four measured quantities used to calculate them, namely, the relative current to the target I_1/I_2, the pressure difference $P = P_1 - P_2$, the temperature T, and the effective reaction chamber length z. (I_1 and I_2 are the target currents when the reaction chamber pressures are P_1 and P_2, respectively.) Since

$$\sigma = n^{-1}z^{-1} \ln(I_1/I_2) = kTp^{-1}z^{-1} \ln(I_1/I_2)$$

by taking differentials of both sides of the equation for σ and then dividing by σ, we obtain

$$\frac{\Delta\sigma}{\sigma} = \frac{\Delta T}{T} + \frac{\Delta P}{P} + \frac{\Delta z}{z} + \frac{\Delta \ln(I_1/I_2)}{\ln(I_1/I_2)}$$

The error in the temperature stems mainly from differences in temperature in the reaction region and at the location of the thermometer. This could not have been more than about 1° C, since the sources of temperature gradients (cold traps and hot filaments) were well removed from the reaction region; thus, $\Delta T/T \sim 0.003$.

The error in measuring z, the effective interaction length, is due largely to the uncertainty in the path taken between grid No. 2 and the target. For an ion entering the chamber on the axis, the longest path is to the edge of the target 0.45 inch from the axis, while the shortest is to the center. The difference in path length is about 0.05 inch out of a total length of about 2 inches causing a 2.5-percent uncertainty in path length. The application of an electric field between the target and grid No. 3 shortens the effective value of z by an amount less than 0.02 inch or 1 percent of the total, but this is corrected for in the reported values of σ. Other uncertainties in z result from penetration of potential through grid No. 2 and from a slight curvature in grid No. 3. Both of these could account for an additional 0.5-percent error. The total uncorrectable error in z is thus about 3 percent.

Uncertainty in determining the pressure must be the largest contribution to systematic error. The reading errors of the McLeod gage at typical operating pressures $P_1 = 2.3\times10^{-4}$ torr, $P_2 = 1.2\times10^{-3}$ torr were given by the manufacturer as $\pm2.5\times10^{-6}$ torr and $\pm5.0\times10^{-6}$ torr, respectively. Sticking of the mercury did not appear to be a problem, provided the gage was tapped vigorously before being read. Measurements were quite reproducible (±5 percent) even for different operators. If we add to the McLeod gage reading error of $P = \pm2$ percent, that of the ion gage ±0.02, we get $\Delta P/P = \pm0.04$.

Recently Rothe (ref. 16), and Ishii and Nakayama (ref. 17) reported that the pumping of mercury by the cold trap between the McLeod gage and the vacuum system could lead to an error of up to 25 percent in the pressure calibration when the McLeod gage measurements are taken at room temperature. Our data do not take this effect into account. If one desires to correct our data for this

effect, using the procedure suggested by Ishii and Nakayama, then the cross section values should be reduced by 4 percent.

The uncertainty in the current ratio I_1/I_2 is caused primarily by fluctuations in the beam current. These were larger at lower energies. From the chart recorder records of these currents one obtains $\Delta I_1/I_1 \sim 0.07$ at 0.5 eV, 0.01 at 1 eV, 0.01 at 5 eV, 0.01 at 10 eV with nearly identical values for $\Delta I_2/I_2$. The limits of error (aside from the possible pressure correction due to the pumping of mercury) calculated from the sources discussed are tabulated below as a function of energy:

$\Delta\sigma/\sigma$	E
0.25	0.5 eV
.10	1.0 eV
.10	5.0 eV
.10	10.0 eV

The energy values quoted above are made uncertain by the contact potential differences along the surface of the target. These differences vary about the average surface potential by ±0.1 V or less.

Further Applications and Techniques

The techniques discussed in this report may be extended to other resonant reactions. Nonresonant reactions pose the problem of decreasing cross sections at low energies. As the beam stability and current intensity decrease with decreasing energy, the quantity to be measured gets smaller in contrast to the situation with resonant reactions. In order to study nonresonant reaction at low energies it will be necessary to improve the beam stability.

Increased beam stability will also improve the chances of obtaining angular scattering data from the retarding potential curves. In making current versus retarding potential measurements, the current must remain constant as the voltage is varied. The voltage of the collector may be varied with high speed, provided sufficient current may be collected at each voltage level to be measurable. Using an electron multiplier for detecting very low signal levels is common. Individual ions are detected and counted. An apparatus of modified design is being built to incorporate such a low level detector. Data taken with this kind of apparatus should be less sensitive to beam fluctuations, since the retarding potentials can be varied much faster than the beam fluctuates.

CONCLUSION

A new method of measuring cross sections for charge exchange and elastic scattering at energies down to 0.5 eV has been described and tested.

Charge exchange cross sections, σ, have been measured for argon ions in argon and nitrogen molecular ions in nitrogen at energies, E, between 0.5 and 17 eV. The argon cross sections are described by the relation

$$\sigma^{1/2} = a - b \ln E$$

with $a = 7.49 \times 10^{-8}$ cm, $b = 0.73 \times 10^{-8}$ cm and E in eV. This is in agreement with the work of other investigators. The nitrogen cross sections are described approximately by the same relation but with $a = 6.48 \times 10^{-8}$ cm, and $b = 0.24 \times 10^{-8}$ cm. The nitrogen cross sections differ slightly from the values given by this relation at 8.5 eV and are considerably larger below 3 eV. At 1 eV our data yield a cross section of 59×10^{-16} cm^2 compared to the logarithmically extrapolated value of 42×10^{-16} cm^2.

While no analysis was made of the fraction of excited molecular nitrogen ions, a hump in the cross section versus energy curve appears to be associated with the presence of vibrationally excited states in the ion beam.

Ames Research Center
National Aeronautics and Space Administration
Moffett Field, Calif., Oct. 19, 1965

APPENDIX

SYMBOLS

a,b	constants
C	calibration constant
E	energy
$E_a(1)$	axial kinetic energy of incident particle before collision
$E_a'(1)$	axial kinetic energy of incident particle after collision
$E_a'(2)$	axial kinetic energy of struck particle after collision
$E_t'(1)$	transverse kinetic energy of incident particle after collision
$E_t'(2)$	transverse kinetic energy of struck particle after collision
h	Planck's constant
I_o	current into entrance of the reaction chamber
I_1	target current when pressure is P_1
I_2	target current when pressure is P_2
I_f	fast ion current reaching target
I_s	current to target due to 1/2 the slow ions formed by charge exchange
k	Boltzmann's constant
l	adiabatic parameter (experimentally determined constant)
ln	natural logarithm
m	mass
n	number of molecules per unit volume in reaction chamber
p	momentum
P	absolute pressure in reaction chamber
P_1P_2	values of pressure in reaction chamber
$P_a(1)$	axial momentum of incident particle before collision

$P_a'(1)$	axial momentum of incident particle after collision
$P_a'(2)$	axial momentum of struck particle after collision
$P_t'(1)$	transverse momentum of incident particle after collision
$P_t'(2)$	transverse momentum of struck particle after collision
Q	ratio of axial kinetic energy of incident particle before collision to that after the collision
R	ratio of axial kinetic energy of struck particle after collision to that of incident particle before the collision
T	absolute temperature in reaction chamber
torr	pressure exerted by 1 mm Hg at 273° K
v	velocity
V_t	target voltage with respect to reaction chamber
z	effective path length of ions in the thermal gas
δE	change in internal energy of a system resulting from a reaction
Δ	differential operator
θ_{min}	minimum scattering angle experienced by an incident particle such that its final axial kinetic energy is less than 0.1 eV
θ_{max}	maximum angle of deflection experienced by incident particle in a collision such that the axially directed energy of the struck particle after collision is less than 0.1 eV
ν	vibrational quantum number
σ	charge exchange cross section

REFERENCES

1. Mason, Edward A.; Vanderslice, Joseph T.; and Yos, Jerrold M.: Transport Properties of High-Temperature Multicomponent Gas Mixtures. Physics of Fluids, vol. 2, no. 6, Nov. - Dec. 1959, pp. 688-694.

2. McDaniel, Earl W.: Collision Phenomena in Ionized Gases. John Wiley and Sons, Inc., 1964.

3. Hasted, J. B.: Physics of Atom Collisions. Butterworths (London), 1964.

4. Rapp, Donald; and Francis, W. E.: Charge Exchange Between Gaseous Ions and Atoms. J. Chem. Phys., vol. 37, no. 11, Dec. 1, 1962, pp. 2631-2645.

5. Iovitsu, I. Popeseu; and Ionescu-Pallas, N.: Resonant Charge-Exchange and the Kinetics of Ions. Soviet Phys. - Tech. Phys., vol. 4, no. 7, Jan. 1960, pp. 781-791.

6. Dalgarno, A.: The Mobilities of Ions in Their Parent Gases. Phil. Trans. Roy. Soc. London, Series A., vol. 250, no. 982, April 1958, pp. 426-429.

7. Herring, Conyers; and Nichols, M. H.: Thermionic Emission. Rev. Mod. Phys., vol. 21, April 1949, pp. 185-270.

8. Amme, R. C.; and Utterback, N. G.: Effects of Ion Beam Excitation on Charge Transfer Cross Sections Measurements. Atomic Collision Processes, M. R. C. McDowell, ed., North-Holland Pub. Co., Amsterdam, 1964, pp. 847-853.

9. Amme, Robert C.; and Hayden, Howard C.: Ion-Beam Excitation Effects on the Single Charge Transfer Between Argon and Nitrogen. J. Chem. Phys., vol. 42, no. 6, March 15, 1965, pp. 2011-2015.

10. Carlston, C. E.; and Magnuson, G. D.: High Efficiency Low-Pressure Ion Source. Rev. Sci. Inst., vol. 33, no. 9, Sept. 1962, pp. 905-911.

11. Potter, Roy F.: Cross Sections for Charge Transfer Collisions of Low-Energy Ions in N_2 and O_2. J. Chem. Phys., vol. 22, no. 6, June 1954, pp. 974-979.

12. Cramer, W. H.: Elastic and Inelastic Scattering of Low-Velocity Ions: Ne^+ in A, A^+ in Ne, and A^+ in A. J. Chem. Phys., vol. 30, no. 3, March 1959, pp. 641-642.

13. Hasted, J. B.: The Exchange of Charge Between Ions and Atoms. Proc. Roy. Soc. London, Series A, vol. 205, no. 1082, Feb. 1951, pp. 421-438.

14. Stebbings, R. F.; Turner, Ben R.; and Smith, A. C. H.: Charge Transfer in Oxygen, Nitrogen, and Nitric Oxide. J. Chem. Phys., vol. 38, no. 9, May 1963, pp. 2277-2279.

15. McGowan, J. W.; Marmet, P.; and Kerwin, L.: Concerning the Measurement of Charge Transfer Reaction Cross Sections at Thermal Energies. Atomic Collision Processes, M. R. C. McDowell, ed., North-Holland Pub. Co., Amsterdam, 1964, pp. 854-861.

16. Rothe, Erhard W.: Avoiding Erroneous Submicron Pressure Readings: A Refrigerated McLeod. J. Vac. Sci. and Tech., vol. 1, no. 2, Nov. - Dec. 1964, pp. 66-68.

17. Ishii, Hiroshi; and Nakayama, Katsuya: A Serious Error Caused by Mercury Vapor Stream in the Measurement with a McLeod Gauge in the Cold Trap System (Effect of the Diffusion of Nitrogen in the Mercury Vapor Stream). Trans. 8th National Vac. Symposium, vol. 1, 1961, pp. 519-524.

TABLE I.- MAXIMUM ANGLE OF DEFLECTION OF INCIDENT IONS SUCH THAT $E_a'(2) \leq 0.1$ eV

$E_a(1)$, eV	R	$p_t'(1)/p_a'(1)$	θ_{max}, deg
0.5	0.2	0.90	42
1.0	.1	.68	34.2
2.0	.05	.537	28.3
5.0	.02	.405	22.0
10.0	.01	.333	18.4
20.0	.005	.309	17.2

TABLE II.- CHARGE EXCHANGE CROSS SECTIONS σ AS A FUNCTION OF ENERGY E FOR A^+ IONS INCIDENT ON ARGON GAS

E, eV	σ, 10^{-16} cm^2	E, eV	σ, 10^{-16} cm^2
17.0	32.9	5.5	43.1
16.5	25.2	4.9	41.7
15.1	30.5	4.5	46.2
14.0	35.3	4.3	43.7
13.9	29.0	3.7	40.0
13.0	30.1	3.5	48.3
12.0	32.5	2.3	47.6
12.0	35.3	2.2	47.9
10.8	35.4	2.9	41.7
10.7	36.8	1.6	50.4
9.7	30.1	1.0	51.4
9.1	39.2	0.4	65.0
9.0	41.7		
8.5	28.8		
8.0	39.6		
7.9	31.5		
6.7	35.3		
6.1	38.2		
5.5	35.4		

TABLE III.- CHARGE EXCHANGE CROSS SECTIONS σ AS A FUNCTION OF ENERGY E FOR N_2^+ IONS INCIDENT ON NITROGEN GAS

E, eV	σ, 10^{-16} cm^2	E, eV	σ, 10^{-16} cm^2
16.7	34.8	5.8	33.7
16.0	35.1	5.6	34.7
14.6	35.2	5.0	35.7
13.8	35.3	4.6	36.2
12.0	33.0	4.5	34.9
11.8	34.4	4.0	37.2
10.8	35.1	3.6	37.6
10.6	34.8	3.4	37.8
10.2	34.6	3.0	39.0
9.7	36.2	2.6	40.0
9.5	36.6	2.4	44.1
9.0	36.9	2.0	42.5
8.8	37.0	1.5	46.5
8.4	36.4	1.3	57.7
7.9	34.2	1.2	51.8
7.7	37.2	0.8	65.8
7.2	34.5	0.5	96.7
6.8	33.5		
6.7	32.7		
6.1	34.7		

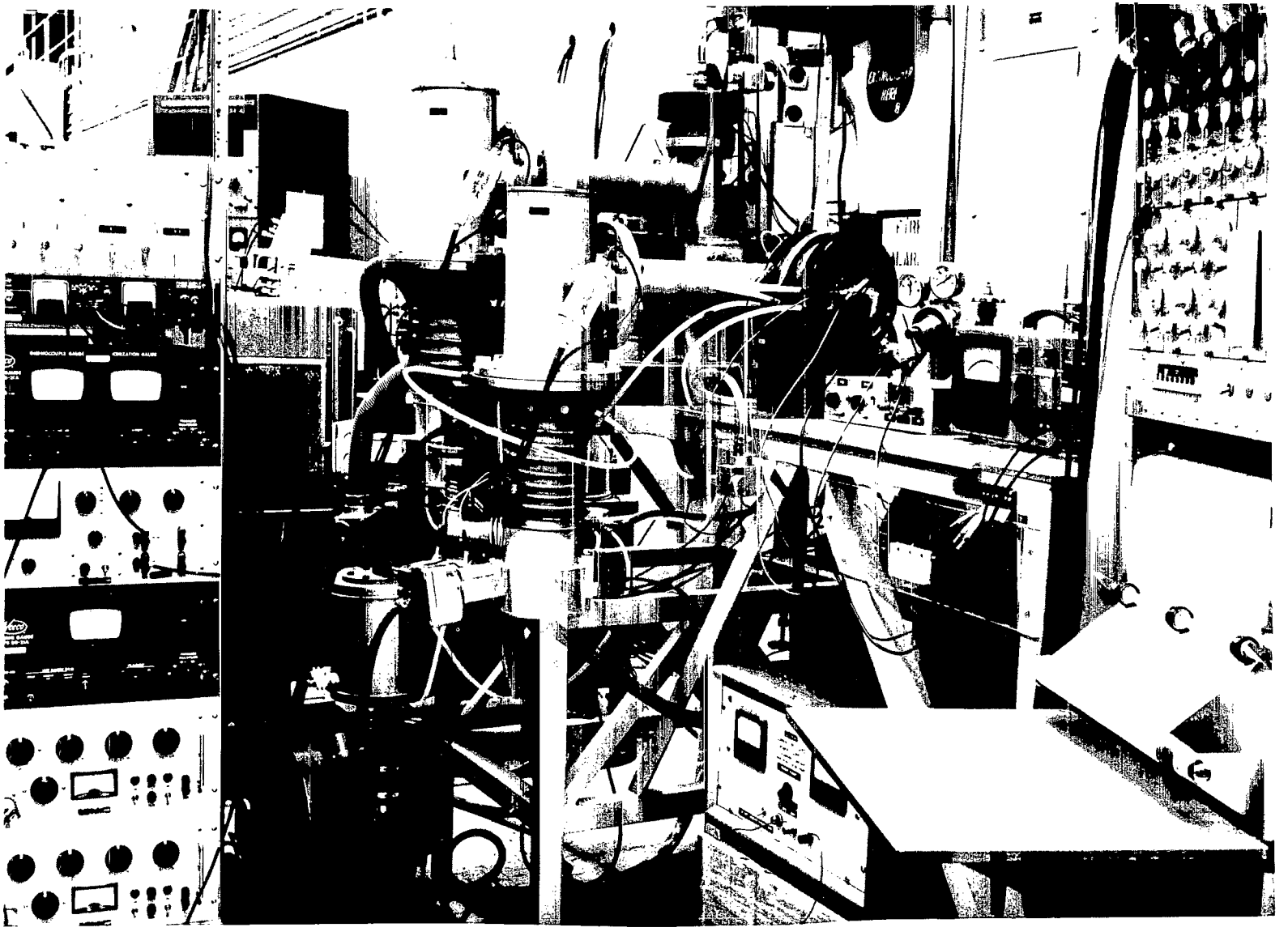

A-34133

Figure 1.- Ion beam accelerator.

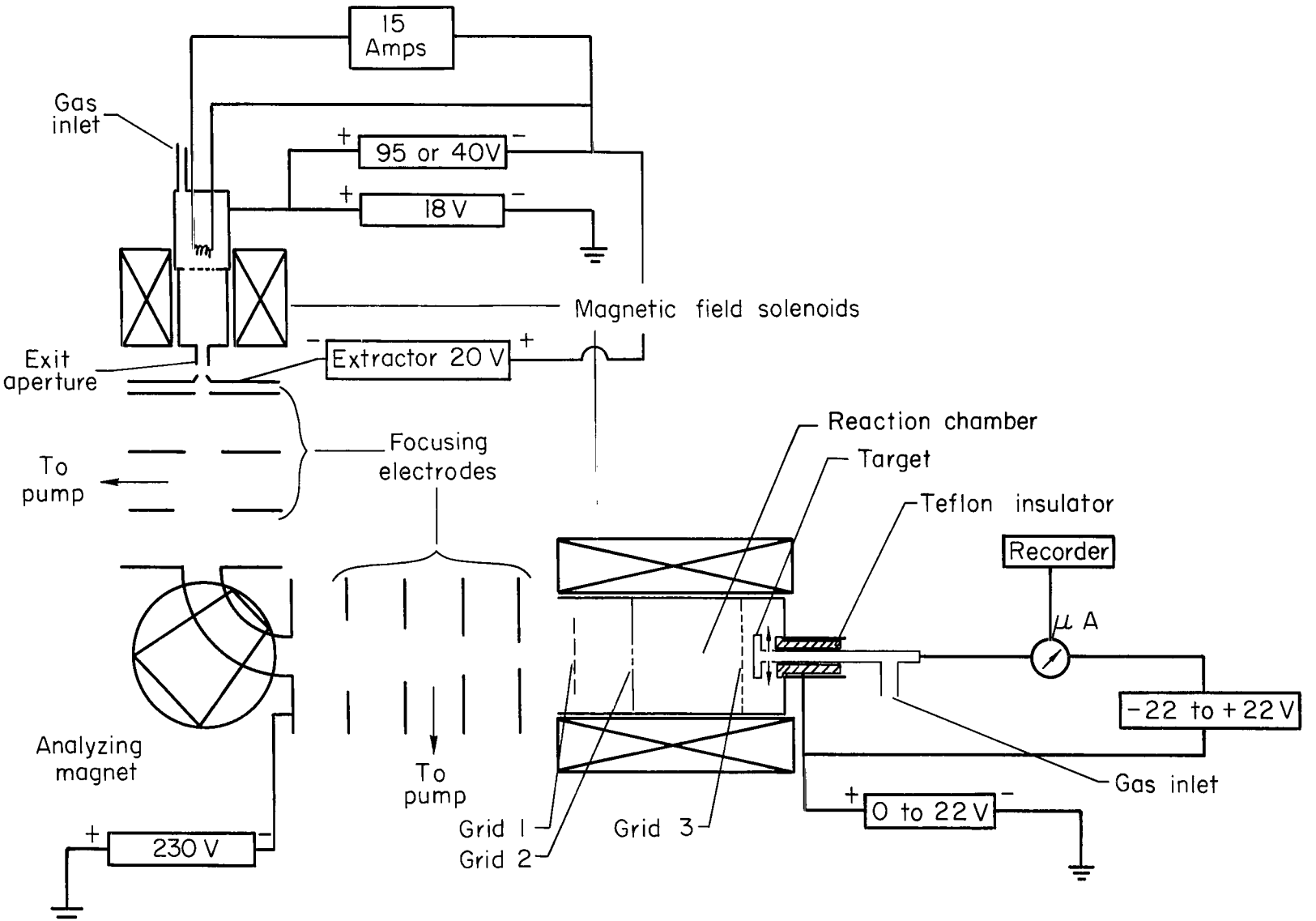

Figure 2.- Schematic diagram of ion accelerator.

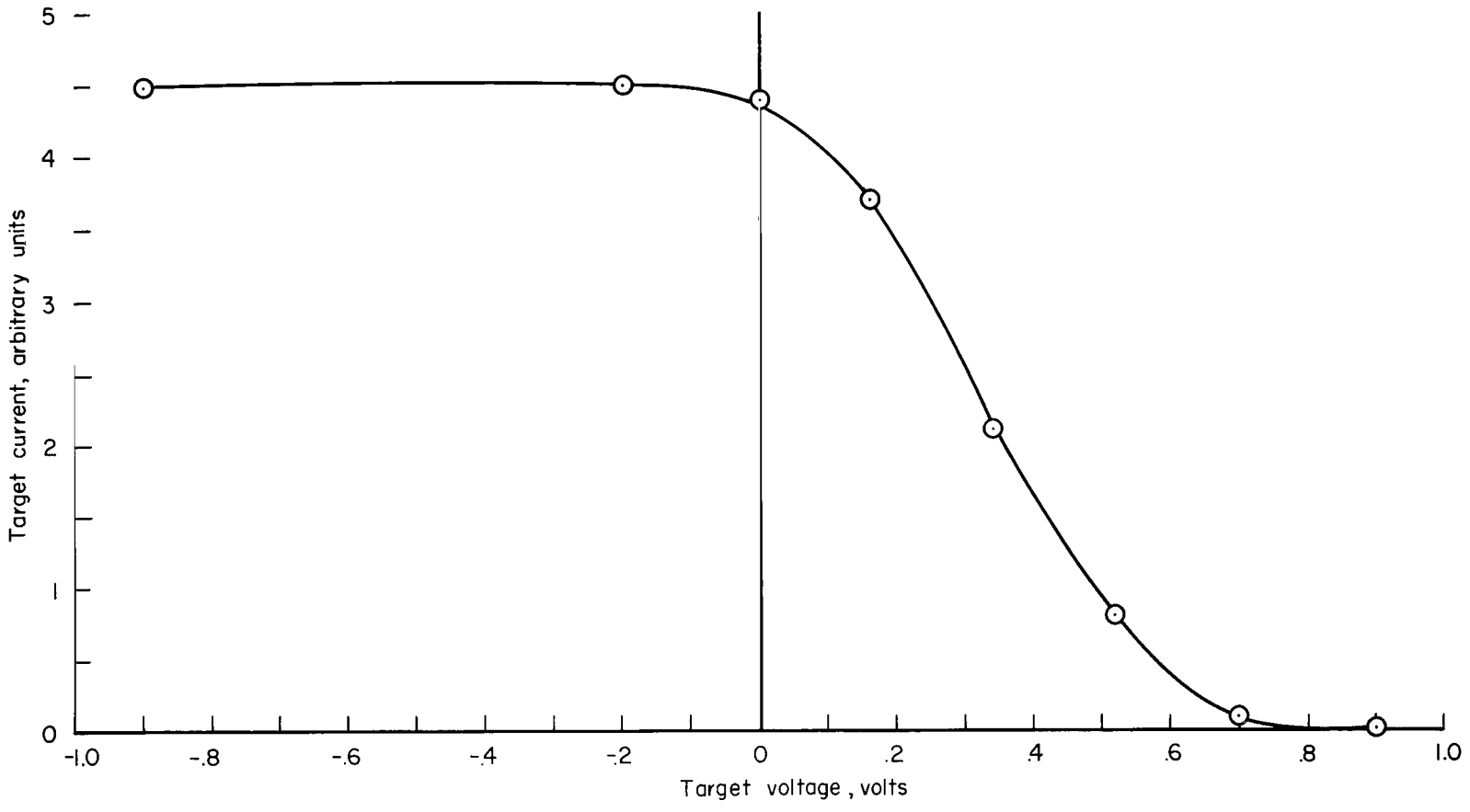

Figure 3.- Target current as a function of target voltage relative to source voltage.

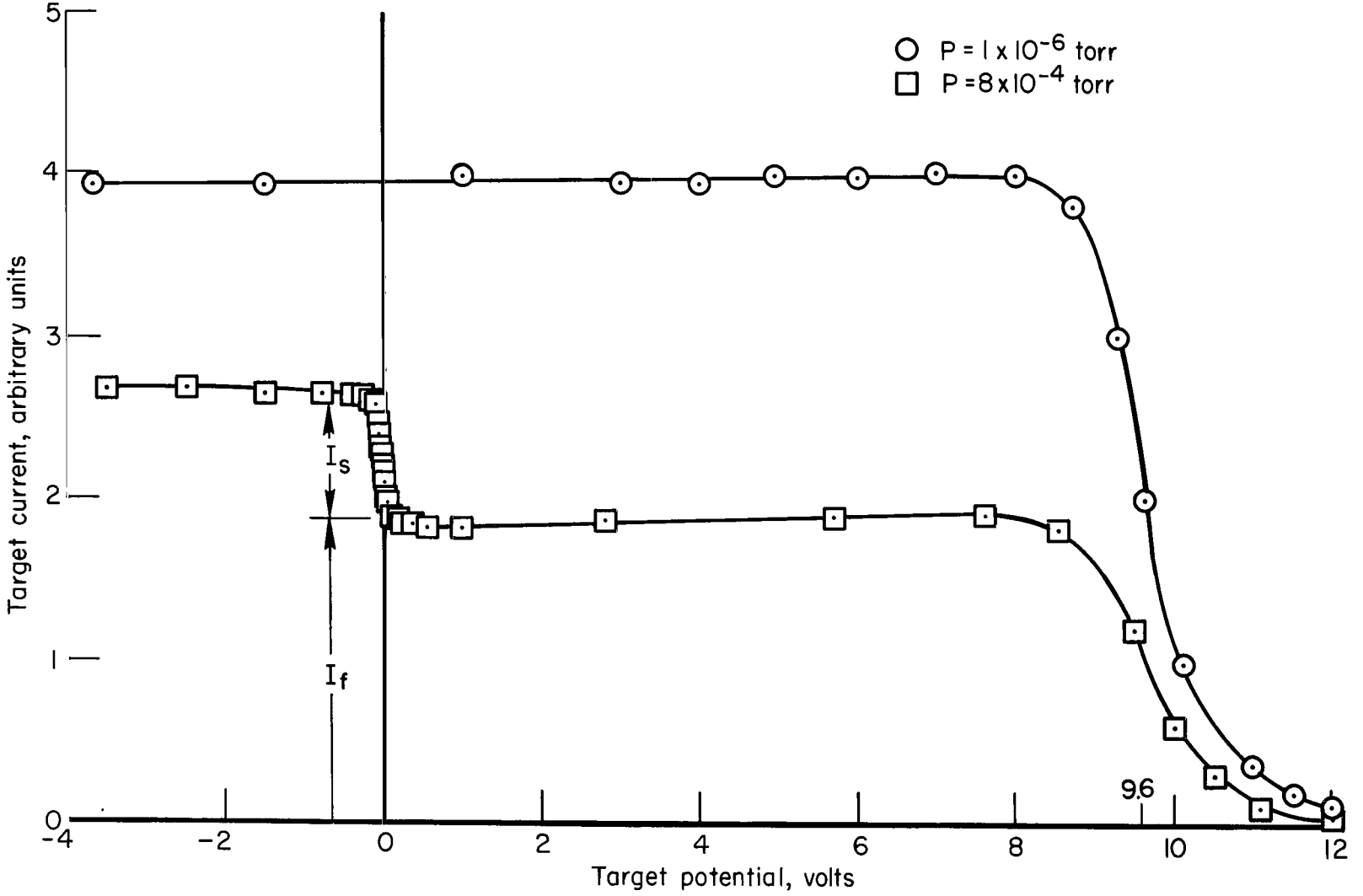

(a) Effect of different pressures.

Figure 4.- Target current as a function of target potential relative to reaction chamber potential.

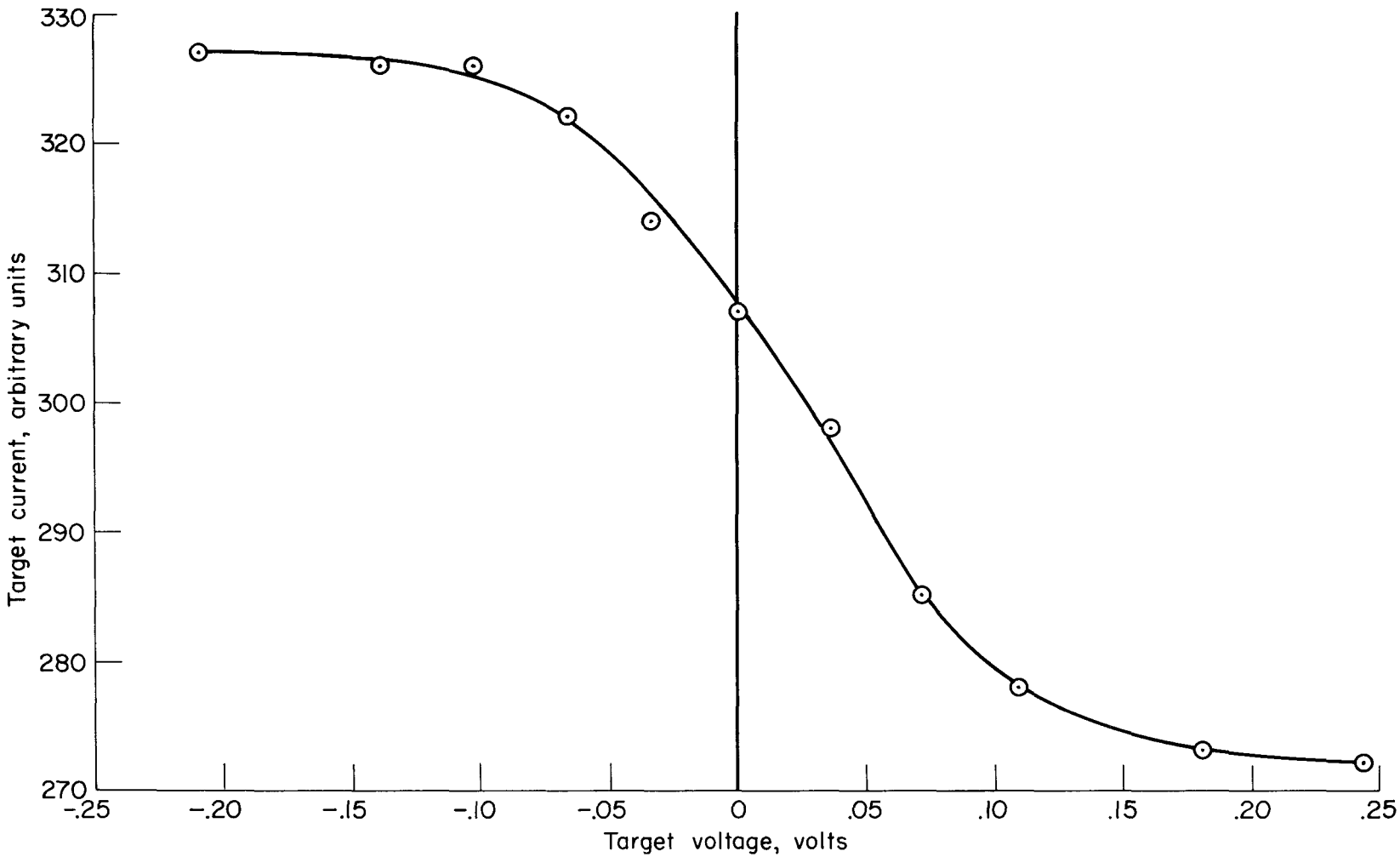

(b) Enlarged plot of retardation of thermal ions.

Figure 4.- Concluded.

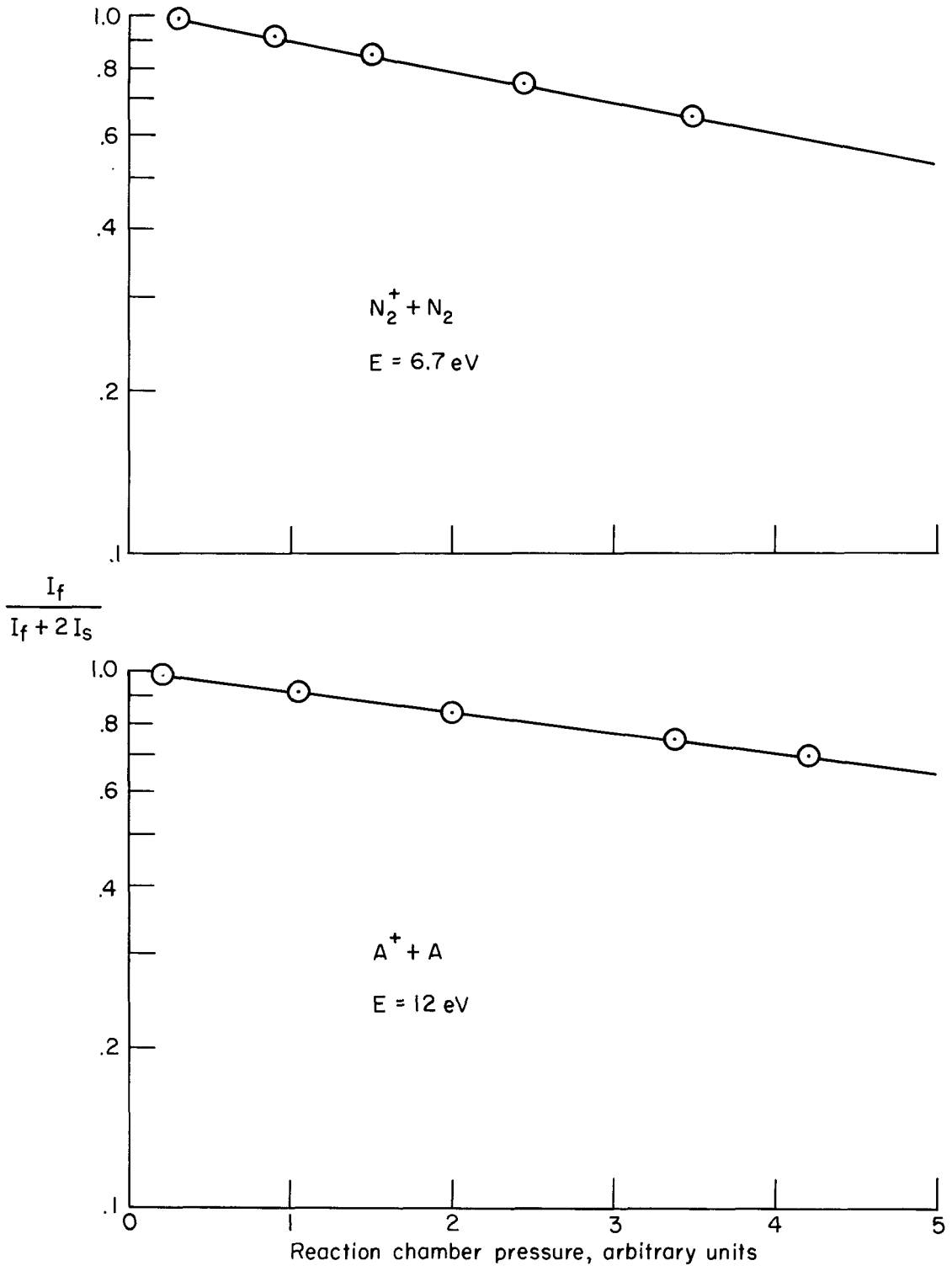

Figure 5.- Target current attenuation, due to admission of gas to the reaction chamber, as a function of reaction chamber pressure.

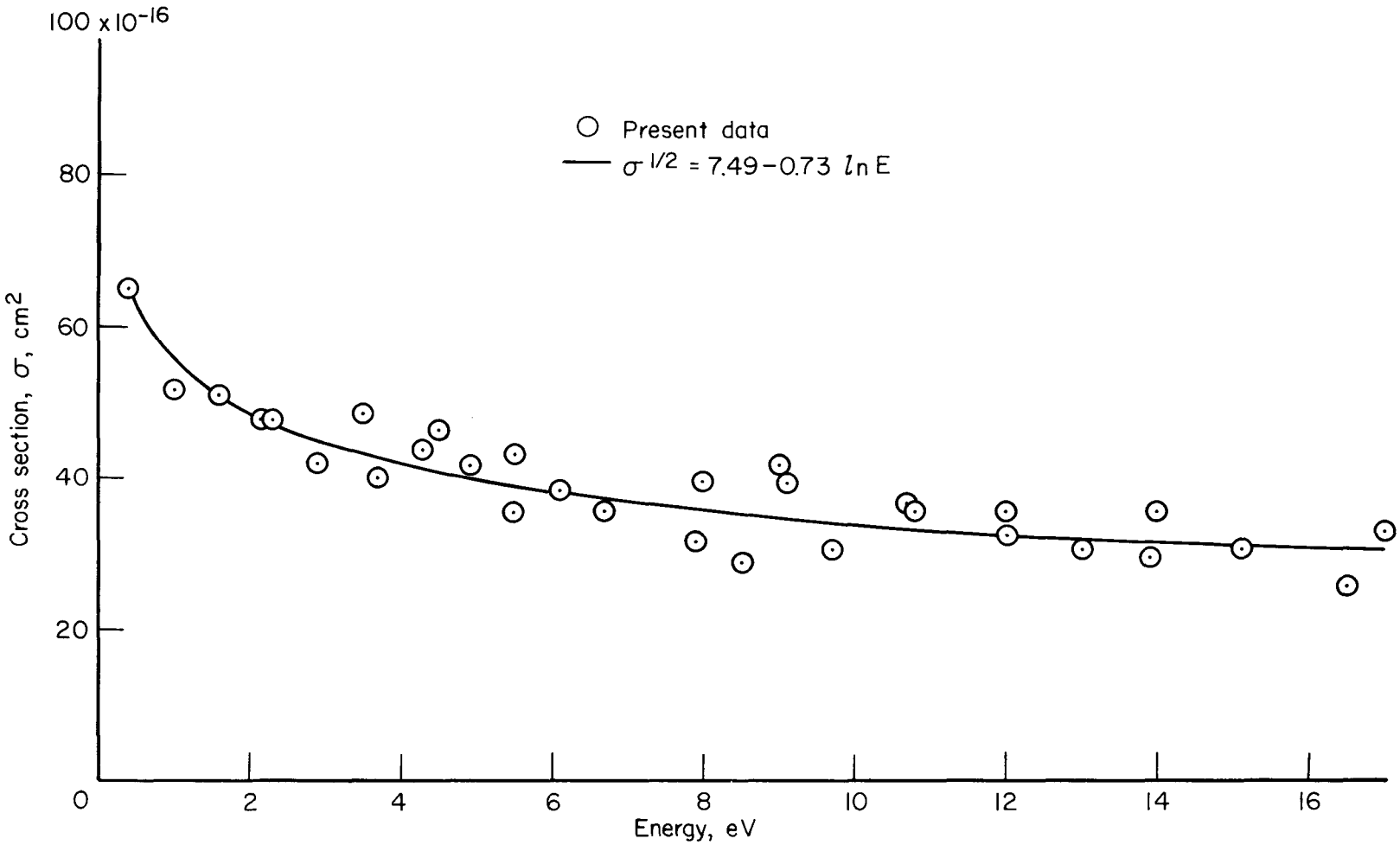

(a) Linear energy scale.

Figure 6.- Charge exchange cross section as a function of energy for A^+ ions incident on argon gas.

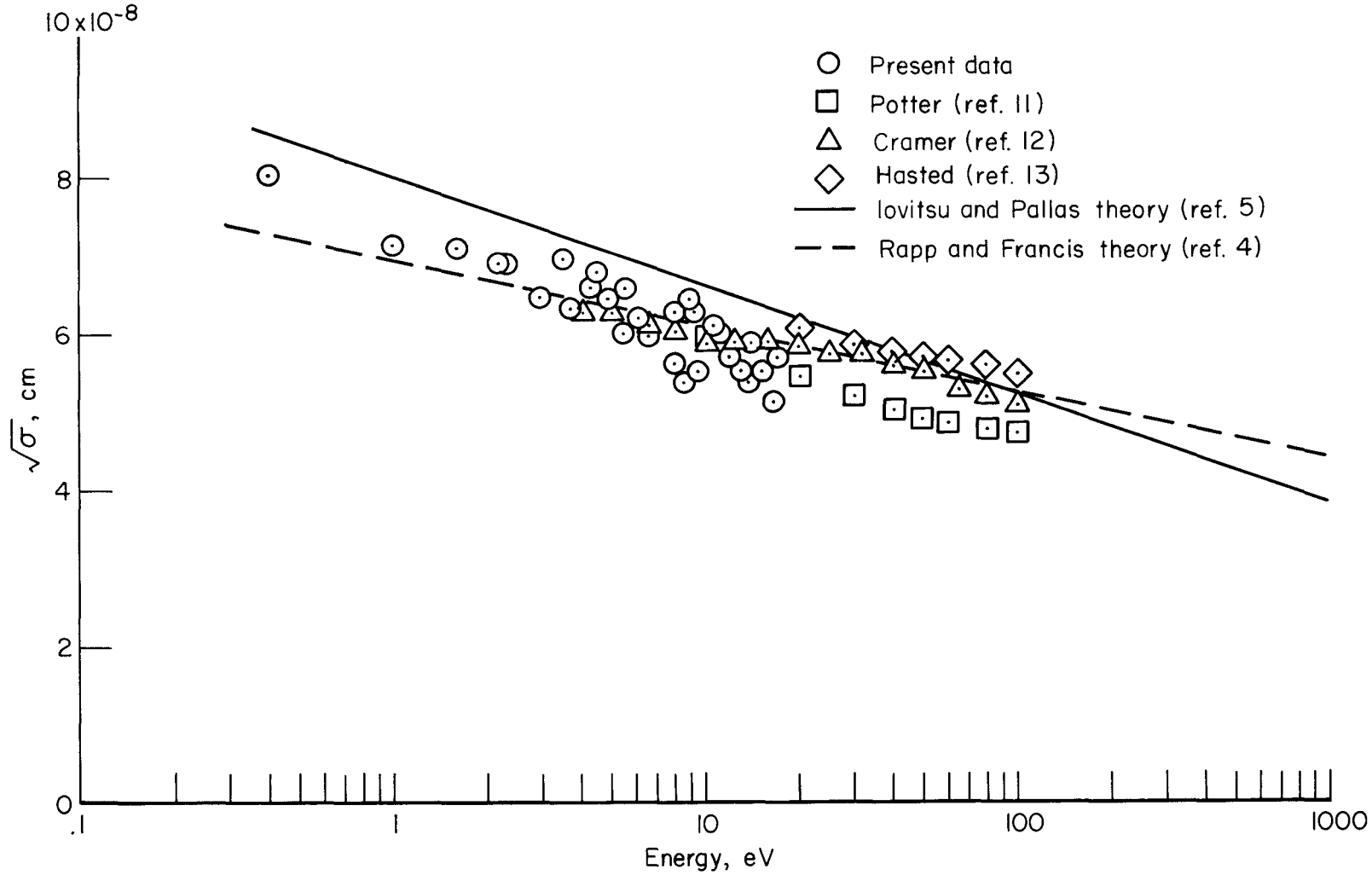

(b) Logarithmic energy scale.

Figure 6.- Concluded.

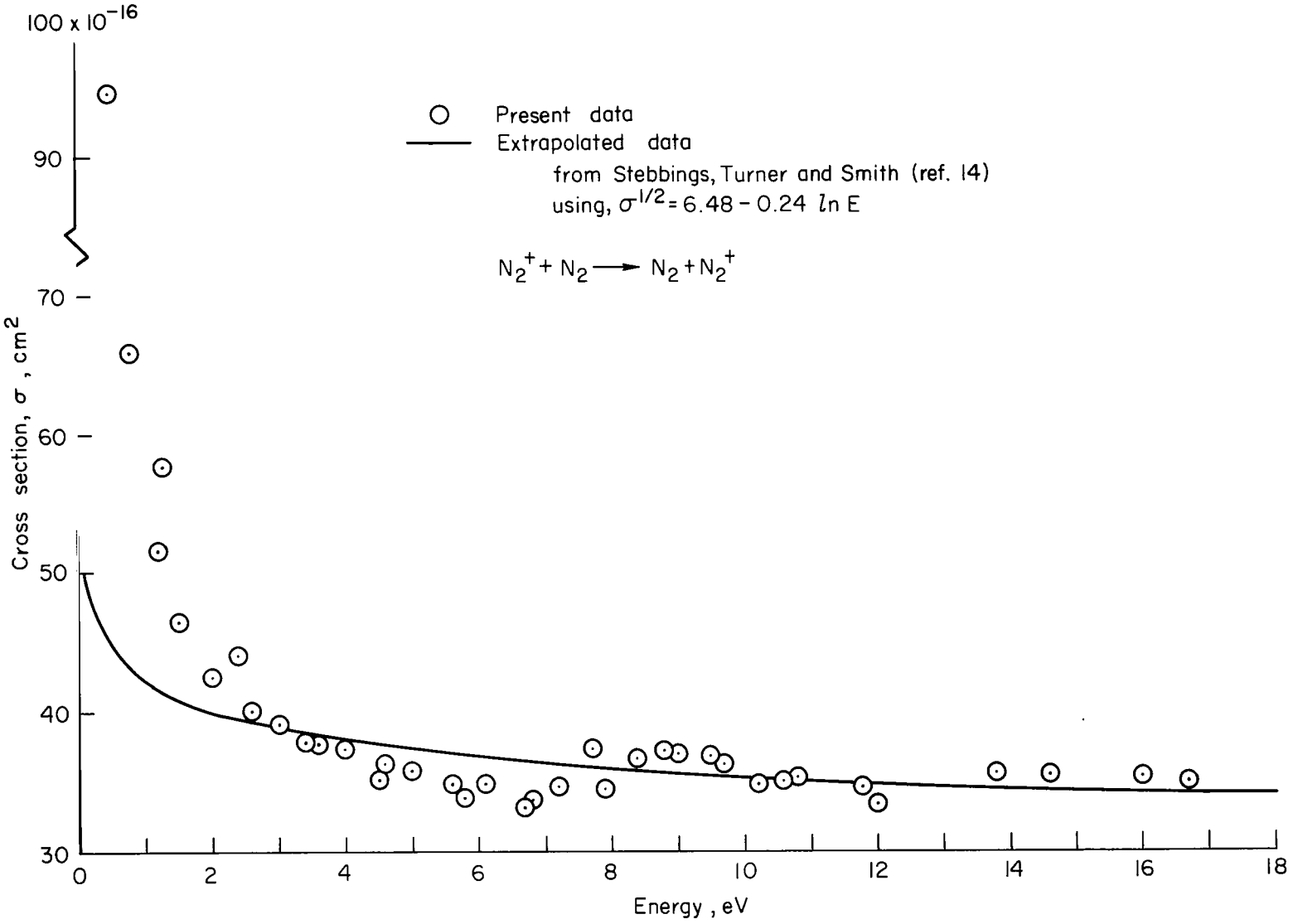

(a) Linear energy scale.

Figure 7.- Charge exchange cross section as a function of energy for N_2^+ ions incident on nitrogen gas.

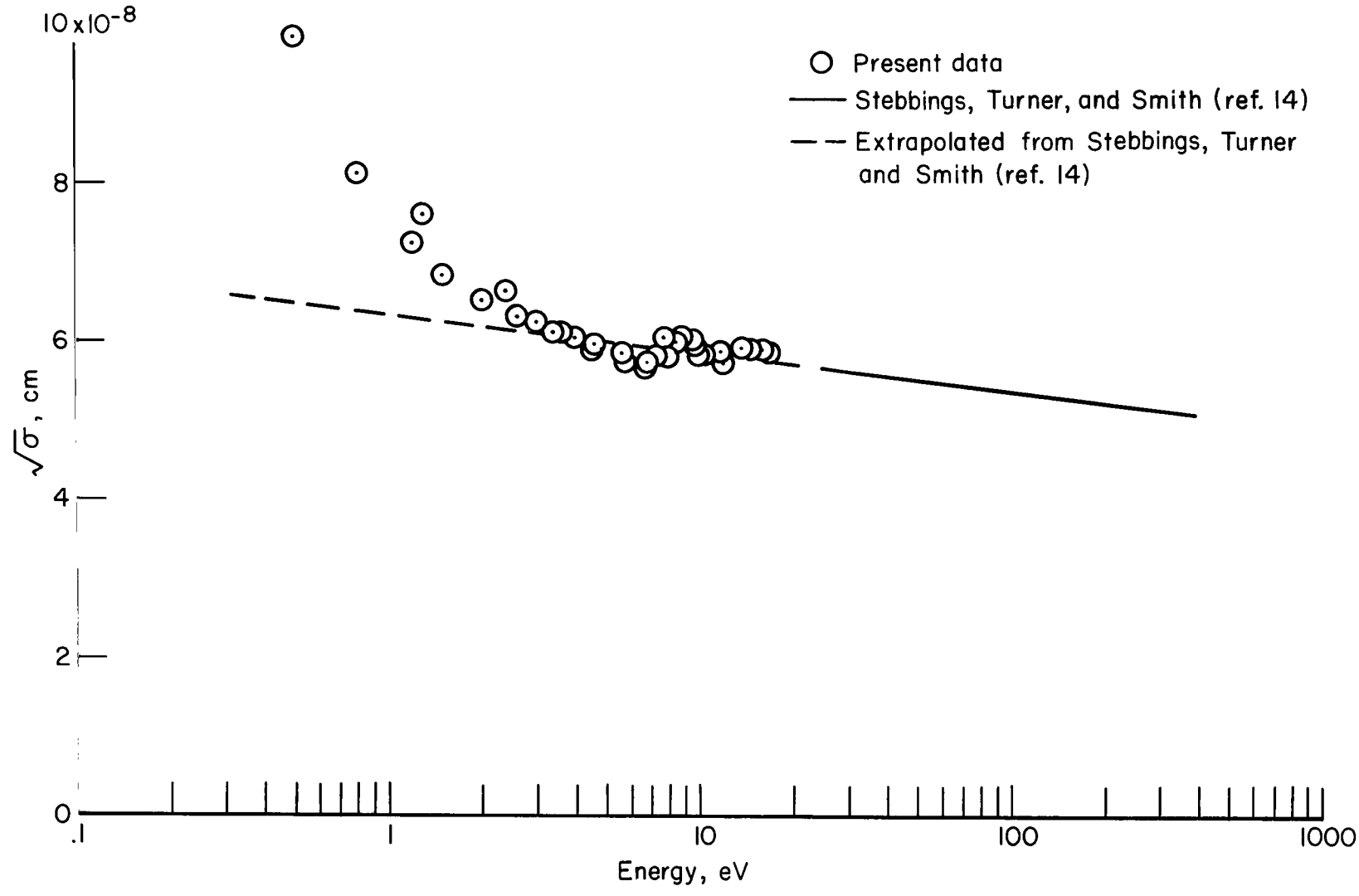

(b) Logarithmic energy scale.

Figure 7.- Concluded.

"The aeronautical and space activities of the United States shall be conducted so as to contribute . . . to the expansion of human knowledge of phenomena in the atmosphere and space. The Administration shall provide for the widest practicable and appropriate dissemination of information concerning its activities and the results thereof."

—NATIONAL AERONAUTICS AND SPACE ACT OF 1958

NASA SCIENTIFIC AND TECHNICAL PUBLICATIONS

TECHNICAL REPORTS: Scientific and technical information considered important, complete, and a lasting contribution to existing knowledge.

TECHNICAL NOTES: Information less broad in scope but nevertheless of importance as a contribution to existing knowledge.

TECHNICAL MEMORANDUMS: Information receiving limited distribution because of preliminary data, security classification, or other reasons.

CONTRACTOR REPORTS: Technical information generated in connection with a NASA contract or grant and released under NASA auspices.

TECHNICAL TRANSLATIONS: Information published in a foreign language considered to merit NASA distribution in English.

TECHNICAL REPRINTS: Information derived from NASA activities and initially published in the form of journal articles.

SPECIAL PUBLICATIONS: Information derived from or of value to NASA activities but not necessarily reporting the results of individual NASA-programmed scientific efforts. Publications include conference proceedings, monographs, data compilations, handbooks, sourcebooks, and special bibliographies.

Details on the availability of these publications may be obtained from:

SCIENTIFIC AND TECHNICAL INFORMATION DIVISION

NATIONAL AERONAUTICS AND SPACE ADMINISTRATION

Washington, D.C. 20546